General Disclaimer

One or more of the Following Statements may affect this Document

- This document has been reproduced from the best copy furnished by the organizational source. It is being released in the interest of making available as much information as possible.

- This document may contain data, which exceeds the sheet parameters. It was furnished in this condition by the organizational source and is the best copy available.

- This document may contain tone-on-tone or color graphs, charts and/or pictures, which have been reproduced in black and white.

- This document is paginated as submitted by the original source.

- Portions of this document are not fully legible due to the historical nature of some of the material. However, it is the best reproduction available from the original submission.

NASA Technical Memorandum 86984

Calculation of Three-Dimensional, Viscous Flow Through Turbomachinery Blade Passages by Parabolic Marching

Theodore Katsanis
Lewis Research Center
Cleveland, Ohio

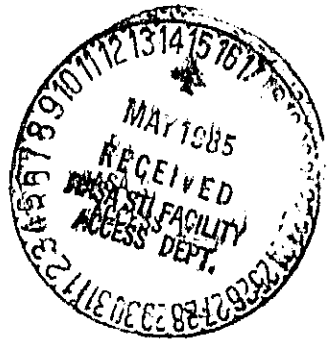

Prepared for the
Twenty-first Joint Propulsion Conference
cosponsored by the AIAA, SAE, and ASME
Monterey, California, July 8-11, 1985

NASA

CALCULATION OF THREE-DIMENSIONAL, VISCOUS FLOW THROUGH TURBOMACHINERY BLADE PASSAGES BY PARABOLIC MARCHING

Theodore Katsanis
National Aeronautics and Space Administration
Lewis Research Center
Cleveland, Ohio 44135

SUMMARY

The three-dimensional compressible Navier-Stokes equations are formulated in a rotating coordinate system, so as to include centrifugal and Coriolis forces. The equations are parabolized by using a previously calculated inviscid static pressure field. The thin layer Navier-Stokes approximation, which neglects streamwise diffusion, is used. A body-fitted coordinate system is used. The streamwise momentum equation is uncoupled from the cross-stream momentum equation by using contravariant momentum components, and then using the contravariant velocity components as primary unknowns. To reduce problems with small separated regions, the Reyhner and Flugge-Lotz approximation is used. The energy equation is included to allow for calculation of heat transfer. The flow may be laminar, or a simple eddy-viscosity turbulence may be used. A number of curved ducts and an axial stator have been analyzed, including cases for which experimental data are available.

NOMENCLATURE

e total internal energy

H total enthalpy

I rothalpy

J transformation Jacobian from Cartesian to (ξ,η,ζ) coordinates

J_1 transformation Jacobian from Cartesian to cylindrical coordinates

J_2 transformation Jacobian from cylindrical to (ξ,η,ζ) coordinates

k thermal conductivity

p pressure

r radius

t time

V absolute velocity

W relative velocity

x cartesian coordinate

y cartesian coordinate

z cartesian coordinate

γ specific heat ratio

ζ hub-to-shroud grid coordinate

η blade-to-blade grid coordinate

θ angular coordinate, radians

μ viscosity

ξ streamwise grid coordinate

ρ density

τ stress

ω angular velocity

Subscripts:

r r component

z z component

θ θ component

Superscripts:

ζ ζ contravariant component

η η contravariant component

ξ ξ contravariant component

INTRODUCTION

Well-guided internal flow without separated regions behaves in a parabolic manner (ref. 1) so that the flow field can be predicted using a parabolic, streamwise marching method. Several computer codes have been written for calculating three-dimensional viscous flow through ducts of fairly complex geometry (ref. 2 and 3). The same principles can be applied to calculate flow through the blades of a turbomachine. However, there are several distinguishing aspects of flow through a turbomachine blade row: (1) The blade row may be rotating. (2) The hub and shroud are usually surfaces of revolution. (3) The passage has four walls meeting at an angle. (4) The flow may be periodic upstream and downstream of the blade. (5) The shroud is usually stationary for a rotating blade row. The method and computer code described here is especially formulated to satisfy and take advantage of these particular aspects of the flow.

The parabolic marching calculation is analagous to calculation of a three-dimensional boundary layer. An inviscid pressure field is used as an initial pressure field; then a single-pass calculation through the length of the blade passage is made. To simplify the application of boundary conditions on complex blade surfaces, a body-fitted coordinate system is used. This body-fitted coordinate system has one coordinate which generates circles about the axis of rotation. One of the coordinate surfaces coincides with the hub of the blade row, and another coincides with the shroud. This type of coordinate system eases implementation of periodic boundary conditions upstream and downstream of the blade row; on the other hand, this type of coordinate system cannot be orthogonal.

In the spirit of Patankar and Spalding (ref. 1) the streamwise momentum calculation is uncoupled from the cross-stream momentum calculation. This uncoupling is accomplished by using contravariant components of the momentum equation, and using contravariant velocity components as the primary unknowns. The downstream contravariant velocity components are always calculated implicitly for stability. To calculate the streamwise contravariant velocity components at the next downstream station, it is assumed that the static pressure and cross-stream contravariant velocity components are known at the previous upstream station. The streamwise pressure gradient is varied by a constant amount over the passage cross-section so that global mass flow through the entire passage is conserved. The cross-stream contravariant velocity components are calculated at the next downstream station based on the inviscid pressure field, and using the last calculated streamwise contravariant velocity components. Continuity is then checked for each mesh region, and the cross-stream pressure gradient is adjusted so that continuity is satisfied for every mesh region. Iteration is required at each station so that both cross-stream momentum and local continuity are satisfied. For turbulent flow, the Baldwin-Lomax eddy-viscosity turbulence model is used (ref. 4).

PARABOLIC MARCHING THROUGH A TURBOMACHINE PASSAGE

Contravariant Form of the Navier-Stokes Equations for a Rotating Non-orthogonal Coordinate System

The continuity equation in conservation form in cylindrical coordinates is:

$$\frac{\partial}{\partial t}(r\rho) + \frac{\partial}{\partial r}(r\rho W_r) + \frac{\partial}{\partial \theta}(\rho W_r) + \frac{\partial}{\partial z}(r\rho W_z) = 0 \qquad (1)$$

In cylindrical (r,θ,z) coordinates the Navier-Stokes equations may be written in conservation form as follows:

$$\frac{\partial}{\partial t}(r\rho V_r) + \frac{\partial}{\partial r}(r\rho V_r^2) + \frac{\partial}{\partial \theta}(\rho V_r V_\theta) + \frac{\partial}{\partial z}(r\rho V_r V_z)$$

$$- \rho V_\theta^2 = \frac{\partial}{\partial r}(r\tau_{rr} - rp) + \frac{\partial}{\partial \theta}(\tau_{r\theta}) + \frac{\partial}{\partial z}(r\tau_{rz}) - \tau_{\theta\theta} + p$$

$$\frac{\partial}{\partial t}(r\rho V_\theta) + \frac{\partial}{\partial r}(r\rho V_r V_\theta) + \frac{\partial}{\partial \theta}(\rho V_\theta^2) + \frac{\partial}{\partial z}(r\rho V_\theta V_z)$$

$$= -\rho V_r V_\theta + \frac{\partial}{\partial r}(r\tau_{r\theta}) + \frac{\partial}{\partial \theta}(\tau_{\theta\theta} - p) + \frac{\partial}{\partial z}(r\tau_{\theta z}) + \tau_{r\theta}$$

$$\frac{\partial}{\partial t}(r\rho V_z) + \frac{\partial}{\partial r}(r\rho V_r V_z) + \frac{\partial}{\partial \theta}(\rho V_\theta V_z) + \frac{\partial}{\partial z}(r\rho V_z^2)$$

$$= \frac{\partial}{\partial r}(r\tau_{rz}) + \frac{\partial}{\partial \theta}(\tau_{r\theta}) + \frac{\partial}{\partial z}(r\tau_{zz} - p)$$

The change to a rotating coordinate system is accomplished by the change of variables:

$$t' = t \qquad W_r = V_r$$

$$r' = r \qquad W_\theta = V_\theta - \omega r$$

$$\theta' = \theta - \omega t \qquad W_z = V_z$$

$$z' = z$$

The partial derivatives with respect to t then become:

$$\frac{\partial}{\partial t} = \frac{\partial}{\partial t'} - \omega \frac{\partial}{\partial \theta}$$

The resulting Navier-Stokes equations for rotating cylindrical coordinates are now (the ' has been dropped):

$$\frac{\partial}{\partial t}(r\rho W_r) + \frac{\partial}{\partial r}(r\rho W_r^2) + \frac{\partial}{\partial \theta}(\rho W_r W_\theta) + \frac{\partial}{\partial z}(r\rho W_r W_z)$$

$$= \rho V_\theta^2 - r\frac{\partial p}{\partial r} - \tau_{\theta\theta} + \frac{\partial}{\partial r}(r\tau_{rr}) + \frac{\partial}{\partial \theta}(\tau_{r\theta}) + \frac{\partial}{\partial z}(r\tau_{rz}) \qquad (2)$$

$$\frac{\partial}{\partial t}(r\rho W_\theta) + \frac{\partial}{\partial r}(r\rho W_\theta W_r) + \frac{\partial}{\partial \theta}(\rho W_\theta^2) + \frac{\partial}{\partial z}(r\rho W_\theta W_z)$$

$$= -\rho W_r (W_\theta + 2\omega r) - \frac{\partial p}{\partial \theta} + \tau_{r\theta} + \frac{\partial}{\partial r}(r\tau_{r\theta})$$

$$+ \frac{\partial}{\partial \theta}(\tau_{\theta\theta}) + \frac{\partial}{\partial z}(r\tau_{r\theta}) \qquad (3)$$

$$\frac{\partial}{\partial t}(r\rho W_z) + \frac{\partial}{\partial r}(r\rho W_z W_r) + \frac{\partial}{\partial \theta}(\rho W_z W_\theta) + \frac{\partial}{\partial z}(r\rho W_z^2)$$

$$= -r\frac{\partial p}{\partial z} + \frac{\partial}{\partial r}(r\tau_{rz}) + \frac{\partial}{\partial \theta}(\tau_{\theta z}) + \frac{\partial}{\partial z}(r\tau_{zz}) \qquad (4)$$

Finally, the energy equation in conservation form is:

$$\frac{\partial e}{\partial t} + \nabla\cdot\left((e + p)\,\bar{V}\right) = \nabla\cdot k\nabla T + \nabla\cdot(\tau\,\bar{V})$$

This is expanded in cylindrical coordinates, and transformed tc rotating coordinates using

$$\frac{\partial}{\partial t} = \frac{\partial}{\partial t'} - \omega\,\frac{\partial}{\partial \theta}$$

Also, rothalpy I is introduced, using the relation

$$e + p = \rho I + \omega r \rho V_\theta$$

The energy equation in conservation form, for rotating cylindrical coordinates and in terms of rothalpy is:

$$\frac{\partial}{\partial t}\left(r(\rho I - p)\right) + r\nabla\cdot(\rho I\bar{W}) = r\nabla\cdot k\nabla T + r\nabla\cdot(\tau\,\bar{W})$$

or

$$\frac{\partial}{\partial t}\left(r(\rho I - p)\right) + \frac{\partial}{\partial r}\,(r\rho I W_r) + \frac{\partial}{\partial \theta}\,(\rho I W_\theta) + \frac{\partial}{\partial z}\,(r\rho I W_z)$$

$$= \frac{\partial}{\partial r}\,(rk\,\frac{\partial T}{\partial r}) + \frac{\partial}{\partial \theta}\,(\frac{k}{r}\,\frac{\partial T}{\partial \theta}) + \frac{\partial}{\partial z}\,(rk\,\frac{\partial T}{\partial z})$$

$$+ \frac{\partial}{\partial r}\left(r(W_r\tau_{rr} + W_\theta\tau_{r\theta} + W_z\tau_{rz})\right) + \frac{\partial}{\partial \theta}\,(W_r\tau_{r\theta} + W_\theta\tau_{\theta\theta}$$

$$+ W_z\tau_{\theta z}) + \frac{\partial}{\partial z}\left(r(W_r\tau_{rz} + W_\theta\tau_{\theta z} + W_z t_{zz})\right) \qquad (5)$$

Equations (1) to (5) can be written in compact form as

$$\partial_t q + \partial_r E + \partial_\theta F + \partial_z G = K + \partial_r R + \partial_\theta S + \partial_z T \qquad (6)$$

where

$$q = r\begin{bmatrix}\rho\\ \rho W_r\\ \rho W_\theta\\ \rho W_z\\ \rho I - p\end{bmatrix} \qquad E = r\begin{bmatrix}\rho W_r\\ \rho W_r^2\\ \rho W_r W_\theta\\ \rho W_r W_z\\ \rho W_r I\end{bmatrix} \qquad F = \begin{bmatrix}\rho W_\theta\\ \rho W_\theta W_r\\ \rho W_\theta^2\\ \rho W_\theta W_z\\ \rho W_\theta I\end{bmatrix}$$

$$G = r\begin{bmatrix} \rho W_z \\ \rho W_z W_r \\ \rho W_z W_\theta \\ \rho W_z^2 \\ \rho W_z I \end{bmatrix} \qquad K = \begin{bmatrix} 0 \\ \rho V_\theta^2 - \frac{r\partial p}{\partial r} - t_{\theta\theta} \\ \tau_{r\theta} - \frac{\partial p}{\partial \theta} - \rho W_r (W_\theta + 2\omega r) \\ -r\frac{\partial p}{\partial z} \\ 0 \end{bmatrix}$$

$$R = r\begin{bmatrix} 0 \\ \tau_{rr} \\ \tau_{r\theta} \\ \tau_{rz} \\ W_r\tau_{rr} + W_\theta\tau_{r\theta} + W_z\tau_{rz} + \frac{k\partial T}{\partial r} \end{bmatrix}$$

$$S = \begin{bmatrix} 0 \\ \tau_{r\theta} \\ \tau_{\theta\theta} \\ \tau_{\theta z} \\ W_r\tau_{r\theta} + W_\theta\tau_{\theta\theta} + W_z\tau_{\theta z} + k\frac{\partial T}{r\partial\theta} \end{bmatrix}$$

$$T = r\begin{bmatrix} 0 \\ \tau_{rz} \\ \tau_{\theta z} \\ t_{zz} \\ W_r\tau_{rz} + W_\theta\tau_{\theta z} + W_z\tau_{zz} + k\frac{\partial T}{\partial z} \end{bmatrix}$$

Equation (6) can be transformed to an arbitrary nonorthogonal rotating coordinate system (ξ, η, ζ) using the chain rule. When this is done, considerable simplification occurs by combining terms properly (refs. 5 and 6), and by using the contravariant velocity components as variables. Note that terms such as

$$\left(\frac{\xi_r}{J_2}\right)_\xi + \left(\frac{\eta_r}{J_2}\right)_\eta + \left(\frac{\zeta_r}{J_2}\right)_\zeta$$

are equal to zero (ref. 7), so that factors like ξ_r/J_2 can be moved inside the derivative. The form of the equations is now:

$$\partial_t \hat{q} + \partial_\xi \hat{E} + \partial_\eta \hat{F} + \partial_\zeta \hat{G} = \hat{K} + \partial_\xi \hat{R} + \partial_\eta \hat{S} + \partial_\zeta \hat{T} \tag{7}$$

where

$$\hat{q} = J^{-1}\begin{bmatrix} \rho \\ \rho W_r \\ \rho W_r \\ \rho W_z \\ \rho I - p \end{bmatrix} \qquad \hat{E} = J^{-1}\begin{bmatrix} \rho W^\xi \\ \rho W^\xi W_r \\ \rho W^\xi W_\theta \\ \rho W^\xi W_z \\ \rho W^\xi I \end{bmatrix}$$

$$\hat{F} = J^{-1}\begin{bmatrix} \rho W^\eta \\ \rho W^\eta W_r \\ \rho W^\eta W_\theta \\ \rho W^\eta W_z \\ \rho W^\eta I \end{bmatrix} \qquad \hat{G} = J^{-1}\begin{bmatrix} \rho W^\zeta \\ \rho W^\zeta W_r \\ \rho W^\zeta W_\theta \\ \rho W^\zeta W_z \\ \rho W^\zeta I \end{bmatrix}$$

$$\hat{R} = J^{-1}\begin{bmatrix} 0 \\ \tau_r^\xi \\ \tau_\theta^\xi \\ \tau_z^\xi \\ \xi_r \beta_r + \dfrac{\xi_\theta \beta_\theta}{r} + \xi_z \beta_z \end{bmatrix} \qquad \hat{S} + J^{-1}\begin{bmatrix} 0 \\ \tau_r^\eta \\ \tau_\theta^\eta \\ \tau_z^\eta \\ \eta_r \beta_r + \dfrac{\eta_\theta \beta_\theta}{r} + \eta_z \beta_z \end{bmatrix}$$

$$\hat{T} = J^{-1}\begin{bmatrix} 0 \\ \tau_r^{\zeta} \\ \tau_r^{\zeta} \\ \tau_z^{\zeta} \\ \zeta_r\beta_r + \dfrac{\zeta_\theta\beta_r}{r} + \zeta_z\beta_z \end{bmatrix} \qquad \hat{K} = J^{-1}\begin{bmatrix} 0 \\ \dfrac{\rho V_\theta^2}{r} - \dfrac{\partial p}{\partial r} - \dfrac{t_{\theta\theta}}{r} \\ \dfrac{\tau_{r\theta}}{r} - \dfrac{\partial p}{r\partial\theta} - \rho W_r \dfrac{(W_\theta + 2W_r)}{r} \\ -\dfrac{\partial p}{\partial z} \\ 0 \end{bmatrix}$$

$$W^{\xi} = \xi_r W_r + \xi_\theta\left(\frac{W_\theta}{r}\right) + \xi_z W_z$$

$$W^{\eta} = \eta_r W_r + \eta_\theta\left(\frac{W_\theta}{r}\right) + \eta_z W_z$$

$$W^{\zeta} = \zeta_r W_r + \zeta_\theta\left(\frac{W_\theta}{r}\right) + \zeta_z W_z$$

$$\tau_r^{\xi} = \xi_r\tau_{rr} + \xi_\theta\left(\frac{\tau_{r\theta}}{\tau}\right) + \xi_z\tau_{rz}$$

$$\tau_\theta^{\xi} = \xi_r\tau_{r\theta} + \xi_\theta\left(\frac{\tau_{\theta\theta}}{r}\right) + \xi_z\tau_{\theta z}$$

$$\tau_z^{\xi} = \xi_r\tau_{rz} + \xi_\theta\left(\frac{\tau_{\theta z}}{r}\right) + \xi_z\tau_{zz}$$

$$\tau_r^{\eta} = \eta_r\tau_{rr} + \eta_\theta\left(\frac{\tau_{\theta r}}{r}\right) + \eta_z\tau_{rz}$$

$$\tau_\theta^{\eta} = \eta_r\tau_{r\theta} + \eta_\theta\left(\frac{\tau_{\theta\theta}}{r}\right) + \eta_z\tau_{\theta z}$$

$$\tau_z^{\eta} = \eta_r\tau_{rz} + \eta_\theta\left(\frac{\tau_{\theta z}}{r}\right) + \eta_z\tau_{zz}$$

$$\tau_r^{\zeta} = \zeta_r\tau_{rr} + \zeta_\theta\left(\frac{\tau_{r\theta}}{r}\right) + \zeta_z\tau_{rz}$$

$$\tau_\theta^{\zeta} = \zeta_r\tau_{r\theta} + \zeta_\theta\left(\frac{\tau_{\theta\theta}}{r}\right) + \zeta_z\tau_{\theta z}$$

$$\tau_z^{\zeta} = \zeta_r\tau_{rz} + \zeta_\theta\left(\frac{\tau_{\theta z}}{r}\right) + \zeta_z\tau_{zz}$$

$$\beta_r = W_r \tau_{rr} + W_\theta \tau_{r\theta} + W_z \tau_{rz} + k \partial_r T$$

$$\beta_\theta = W_r \tau_{r\theta} + W_\theta \tau_{\theta\theta} + W_z \tau_{\theta z} + k \frac{\partial_\theta T}{r}$$

$$\beta_z = W_r \tau_{rz} + W_\theta \tau_{\theta z} + W_z \tau_{zz} + k \partial_z T$$

Equation 7 still has cylindrical momentum components. It is desired to utilize momentum components aligned with the mesh, so that streamwise momentum is easily uncoupled from the cross-stream momentum components. This is accomplished by taking the contravariant momentum components. For example, the contravariant ξ-momentum component is ξ_r(r-momentum) plus η_θ/r(θ-momentum) plus ζ_z(z-momentum). This results in:

$$\partial_t \hat{\hat{q}} + \partial_\xi \hat{\hat{E}} + \partial_\eta \hat{\hat{F}} + \partial_\zeta \hat{\hat{G}} = \partial_\xi \hat{\hat{R}} + \partial_\eta \hat{\hat{S}} + \partial_\zeta \hat{\hat{T}} + \hat{\hat{K}} \qquad (8)$$

where

$$\hat{\hat{q}} = \frac{1}{J} \begin{bmatrix} \rho \\ \rho W^\xi \\ \rho W^\eta \\ \rho W^\zeta \\ \rho I - p \end{bmatrix} \qquad \hat{\hat{E}} = \frac{1}{J} \begin{bmatrix} \rho W^\xi \\ \rho W^\xi W^\xi \\ \rho W^\xi W^\eta \\ \rho W^\xi W^\zeta \\ \rho W^\xi I \end{bmatrix} \qquad \hat{\hat{F}} = \frac{1}{J} \begin{bmatrix} \rho W^\eta \\ \rho W^\eta W^\xi \\ \rho W^\eta W^\eta \\ \rho W^\eta W^\zeta \\ \rho W^\eta I \end{bmatrix}$$

$$\hat{\hat{G}} = \frac{1}{J} \begin{bmatrix} \rho W^\zeta \\ \rho W^\zeta W^\xi \\ \rho W^\zeta W^\eta \\ \rho W^\zeta W^\zeta \\ \rho W^\zeta I \end{bmatrix} \qquad \hat{\hat{R}} = \frac{1}{J} \begin{bmatrix} 0 \\ \xi_r \tau_r^\xi + \frac{\xi_\theta \tau_\theta^\xi}{r} + \xi_z \tau_z^\xi \\ \eta_r \tau_r^\xi + \frac{\eta_\theta \tau_\theta^\xi}{r} + \eta_z \tau_z^\xi \\ \zeta_r \tau_r^\xi + \frac{\zeta_\theta \tau_\theta^\xi}{r} + \zeta_z \tau_z^\xi \\ \xi_r \beta_r + \frac{\xi_\theta \beta_\theta}{r} + \xi_z \beta_z \end{bmatrix}$$

$$\hat{\hat{S}} = \frac{1}{J}\begin{bmatrix} 0 \\ \xi_r \tau_r^{\eta} + \frac{\xi_\theta \tau_\theta^{\eta}}{r} + \xi_z \tau_z^{\eta} \\ \eta_r \tau_r^{\eta} + \frac{\eta_\theta \tau_\theta^{\eta}}{r} + \eta_z \tau_z^{\eta} \\ \zeta_r \tau_r^{\eta} + \frac{\zeta_\theta \tau_\theta^{\eta}}{r} + \zeta_z \tau_z^{\eta} \\ \eta_r \beta_r + \frac{\eta_\theta \beta_\theta}{r} + \eta_z \beta_z \end{bmatrix} \qquad \hat{\hat{T}} = \frac{1}{J}\begin{bmatrix} 0 \\ \xi_r \tau_r^{\zeta} + \frac{\xi_\theta \tau_\theta^{\zeta}}{r} + \xi_z \tau_z^{\zeta} \\ \eta_r \tau_r^{\zeta} + \frac{\eta_\theta \tau_\theta^{\zeta}}{r} + \eta_z \tau_z^{\zeta} \\ \zeta_r \tau_r^{\zeta} + \frac{\zeta_\theta \tau_\theta^{\zeta}}{r} + \zeta_z \tau_z^{\zeta} \\ \zeta_r \beta_r + \frac{\zeta_\theta \beta_\theta}{r} + \zeta_z \beta_z \end{bmatrix}$$

$$\hat{\hat{K}} = \frac{1}{J}\begin{bmatrix} 0 \\ \rho G_{\xi\rho} - g^{\xi\xi} p_\xi - g^{\xi\eta} p_\eta - g^{\xi\zeta} p_\zeta - \frac{\xi_r t_{\theta\theta}}{r} + \frac{\xi_\theta t_{r\theta}}{r^2} \\ \rho G_{\eta\rho} - g^{\eta\xi} p_\xi - g^{\eta\eta} p_\eta - g^{\eta\zeta} p_\zeta - \frac{\eta_r \tau_{\theta\theta}}{r} + \frac{\eta_\theta \tau_{r\theta}}{r^2} \\ \rho G_{\zeta\rho} - g^{\zeta\xi} p_\xi - g^{\zeta\eta} p_\eta - g^{\zeta\zeta} p_\zeta - \frac{\zeta_r \tau_{\theta\theta}}{r} + \frac{\zeta_\theta \tau_{r\theta}}{r^2} \\ 0 \end{bmatrix}$$

$$\begin{aligned} G_{\xi\rho} = {} & W^{\xi}\left((\xi_r)_\xi W_r + \left(\frac{\xi_\theta}{r}\right)_\xi W_\theta + (\xi_z)_\xi W_z\right) \\ & + W^{\eta}\left((\xi_r)_\eta W_r + \left(\frac{\xi_\theta}{r}\right)_\eta W_\theta + (\xi_z)_\eta W_z\right) \\ & + W^{\zeta}\left((\xi_r)_\zeta W_r + \left(\frac{\xi_\theta}{r}\right)_\zeta W_\theta + (\xi_z)_\zeta W_z\right) \\ & + \frac{\xi_r V_\theta^2}{r} - \frac{\xi_\theta}{r^2} W_r (W_\theta + 2\omega r) \end{aligned}$$

$$G_{\eta\rho} = W^{\xi}\left((\eta_r)_{\xi} W_r + \left(\frac{\eta_\theta}{r}\right)_{\xi} W_\theta + (\xi_z)_{\xi} W_z\right)$$
$$+ W^{\eta}\left((\eta_r)_{\eta} W_r + \left(\frac{\eta_\theta}{r}\right)_{\eta} W_\theta + (\xi_z)_{\eta} W_z\right)$$
$$+ W^{\zeta}\left((\eta_r)_{\zeta} W_r + \left(\frac{\eta_\theta}{r}\right)_{\zeta} W_\theta + (\xi_z)_{\zeta} W_z\right)$$
$$+ \frac{\eta_r V_\theta^2}{r} - \frac{\eta_\theta}{r^2} W_r(W_\theta + 2\omega r)$$

$$C_{\zeta\rho} = W^{\zeta}\left((\zeta_r)_{\xi} W_r + \left(\frac{\zeta_\theta}{r}\right)_{\xi} W_\theta + (\zeta_z)_{\xi} W_z\right)$$
$$+ W^{\eta}\left((\zeta_r)_{\eta} W_r + \left(\frac{\zeta_\theta}{r}\right)_{\eta} W_\theta + (\zeta_z)_{\eta} W_z\right)$$
$$+ W^{\zeta}\left((\zeta_r)_{\zeta} W_r + \left(\frac{\zeta_\theta}{r}\right)_{\zeta} W_\theta + (z_z)_{\zeta} W_z\right)$$
$$+ \frac{\zeta_r V_\theta^2}{r} - \frac{\zeta_\theta}{r^2} W_r(W_\theta + 2\omega r)$$

Derivation of the Navier-Stokes Equations for Parabolic Marching Through a Turbomachinery Blade Row

Equation (8) retains all terms from the original Navier-Stokes, continuity, and energy equations for a general non orthogonal rotating coordinate system. Some terms will now be eliminated, or neglected. Only steady relative flow is considered so the time derivatives will be eliminated. Also, the thin layer assumption is made so that all streamwise derivatives of viscous terms will be neglected. Further, the mesh that is used is not completely general, so that certain coordinate derivatives will be eliminated.

The coordinate system used is shown in figure 1. The ξ-coordinate is in the streamwise direction, η is the blade to blade direction, and ζ is from hub-to-shroud. Since the hub and shroud are both usually surfaces of revolution, and to make it easier to apply periodic boundary conditions, the η-coordinate lines will be circular arcs coincident with the θ-coordinate lines. Hence, ξ and ζ are functions of r and z only, and are independent of θ:

$$\xi = \xi(r,z), \qquad \xi_\theta = 0$$

$$\eta = \eta(r,\theta,z)$$

$$\zeta = \zeta(r,z) \qquad \zeta_\theta = 0$$

The required coordinate derivatives, ξ_r, ξ_z, η_r, etc. are calculated from the coordinate derivatives of the inverse transformation, r_ξ, θ_ξ, etc., by the equations:

$$\xi_z = \frac{-r_\zeta}{(r_\xi z_\zeta - r_\zeta z_\xi)} \qquad \eta_z = \frac{(r_\zeta \theta_\xi - r_\xi \theta_\zeta)}{\theta_\eta (r_\xi z_\zeta - r_\zeta z_\xi)} \qquad \zeta_z = \frac{r_\xi}{(r_\xi z_\zeta - r_\zeta z_\xi)}$$

$$\xi_\theta = 0 \qquad \eta_\theta = \frac{1}{\theta_\eta} \qquad \zeta_\theta = 0 \tag{9}$$

$$\xi_r = \frac{z_\zeta}{(r_\xi z_\zeta - r_\zeta z_\xi)} \qquad \eta_r = \frac{(\theta_\zeta z_\xi - \theta_\xi z_\zeta)}{\theta_\eta (r_\xi z_\zeta - r_\zeta z_\xi)} \qquad \zeta_r = \frac{-z_\xi}{(r_\xi z_\zeta - r_\zeta z_\xi)}$$

The Jacobian, J, is given by:

$$J = \frac{-1}{r\theta_\eta (r_\xi z_\zeta - r_\zeta z_\xi)} \tag{10}$$

Since ξ is in the streamwise direction, all ξ-derivatives of the viscous terms are neglected. Further, by using the continuity equation, for any function φ, we have:

$$\partial_\xi \left(\rho \frac{W^\xi}{J} \varphi \right) + \partial_\eta \left(\rho \frac{W^\eta}{J} \varphi \right) + \partial_\zeta \left(\rho \frac{W^\zeta}{J} \varphi \right) = \rho \frac{W^\xi}{J} \varphi_\xi + \rho \frac{W^\eta}{J} \varphi_\eta + \rho \frac{W^\zeta}{J} \varphi_\zeta \tag{11}$$

Excluding continuity, the equations become:

$$\rho \frac{W^\xi}{J} \partial_\xi H + \rho \frac{W^\eta}{J} \partial_\eta H + \rho \frac{W^\zeta}{J} \partial_\zeta H = \partial_\eta \tilde{S} + \partial_\zeta \tilde{T} + \tilde{K} \tag{12}$$

where

$$H = \begin{bmatrix} W^\xi \\ W^\eta \\ W^\zeta \\ I \end{bmatrix} \qquad \tilde{S} = J^{-1} \begin{bmatrix} \xi_r \tau_r^\eta + \xi_z \tau_z^\eta \\ \eta_r \tau_r^\eta + \eta_\theta \tau_\theta^\eta / r + \eta_z \tau_z^\eta \\ \zeta_r \tau_r^\eta + \zeta_z \tau_z^\eta \\ \eta_r \beta_r + \eta_\theta \beta_\theta / r + \eta_z \beta_z \end{bmatrix}$$

$$\tilde{T} = J^{-1}\begin{bmatrix} \xi_r \tau_r^{\zeta} + \xi_z \tau_z^{\zeta} \\ \eta_r \tau_r^{\zeta} + \eta_\theta \tau_\theta^{\zeta}/r + \eta_z \tau_z^{\zeta} \\ \zeta_r \tau_r^{\zeta} + \zeta_z \tau_z^{\zeta} \\ \zeta_r \beta_r + \zeta_z \beta_z \end{bmatrix}$$

$$\tilde{K} = J^{-1}\begin{bmatrix} \rho G_{\xi\rho} - g^{\xi\zeta} p_\xi - g^{\xi\eta} p_\eta - g^{\xi\zeta} p_\zeta \\ \rho G_{\eta\rho} - g^{\eta\xi} p_\xi - g^{\eta\eta} p_\eta - g^{\eta\zeta} p_\zeta \\ \rho G_{\zeta\rho} - g^{\zeta\xi} p_\xi - g^{\zeta\eta} p_\eta - g^{\zeta\xi} p_\zeta \\ 0 \end{bmatrix}$$

Consistent with the thin boundary layer assumption, order of magnitude arguments are used to simplify calculation of the stress tensor in terms of the contravariant velocity components. Terms that are important involve the second derivative of a velocity component parallel to a wall with respect to the distance from the same wall, whereas the derivative of a velocity component normal to a wall with respect to the same wall is negligible. Also, coordinate derivatives (ξ_r, η_r, etc.) are considered to vary slowly compared to the velocity components themselves. Even with these simplifications, the calculation of the stress tensor is rather complicated and messy for the non-orthogonal grid used.

Numerical Solution Procedure

A FORTRAN program called PARAMAR has been written to solve equation (12) by parabolic marching. Equation (12) is the thin layer Navier-Stokes equation for a rotating, body fitted coordinate system. The ξ-coordinate is in the streamwise direction, η is blade-to-blade, and ζ is hub-to-shroud, as indicated in figure 1. The equations are parabolized by using a previously calculated inviscid static pressure field, and neglecting streamwise diffusion terms. The pressure field may be obtained by the MERIDL and TSONIC codes (refs. 8 and 9) or from the Denton code (ref. 10).

The form of the three momentum equations and the energy equation is

$$\rho \frac{W^{\xi}}{J}\frac{\partial \varphi}{\partial \xi} + \rho \frac{W^{\eta}}{J}\frac{\partial \varphi}{\partial \eta} + \rho \frac{W^{\zeta}}{J}\frac{\partial \varphi}{\partial \zeta} - \frac{\partial}{\partial \eta}\left(a \frac{\partial \varphi}{\partial \eta}\right) - \frac{\partial}{\partial \zeta}\left(b \frac{\partial \varphi}{\partial \zeta}\right) = S$$

where φ may be any contravariant velocity component or rothalpy. S is the remaining terms of the equation. The coefficients a and b, and the source term S are different for each equation. By using a finite-difference approximation for the ξ-derivative, the equation may be approximated as:

$$\rho \frac{W^{\xi}}{J}(\varphi_{i+1} - \varphi_i) + \rho \frac{W^{\eta}}{J}\left(\frac{\partial \varphi}{\partial \eta}\right)_{i+1} + \rho \frac{W^{\zeta}}{J}\left(\frac{\partial \varphi}{\partial z}\right)_{i+1} - \left(\frac{\partial}{\partial \eta}\left(a \frac{\partial \varphi}{\partial \eta}\right)\right)_{i+1} - \left(\frac{\partial}{\partial \zeta}\left(b \frac{\partial \varphi}{\partial \zeta}\right)\right)_{i+1} = S_i$$

It is assumed that the mesh lines are coordinate lines, and that $\xi_{i+1} - \xi_i = 1$. Similarly, for the other coordinates, it will be assumed that $\Delta\eta = \Delta\zeta = 1$. This equation is an implicit equation for φ_{i+1}. In finite difference form, the equation may be solved for φ_{i+1} directly by using the block tridiagonal algorithm (ref. 11, p. 196)

Because of the importance of accurately calculating continuity for internal flow, a staggered mesh is used, much as suggested by Patankar and Spalding (ref. 1). The mesh arrangement and numbering sheme is shown in figure 2. Each of the momentum equations are uncoupled by using coefficients calculated at the upstream station. Since an inviscid pressure field is used, corrections must be made to account for viscous effects in the boundary layer.

The streamwise (ξ) momentum equation is used to calculate the streamwise contravariant velocity components at the next streamwise station, using zero velocity boundary conditions. After calculating the downstream W^{ξ}, the mass flow at the downstream station will be low due to an increasing displacement thickness of the boundary layer. Hence, the pressure must be reduced at the downstream station, so that global continuity is satisfied. This is done by reducing the stream-wise pressure gradient uniformly over the entire passage cross section.

The cross-stream momentum equations are used to calculate the cross-stream contravariant velocity components at the next station. Zero velocity boundary conditions are used. After calculating the cross-stream velocities, continuity is checked for each mesh region. In general there will not be conservation of mass for each mesh region. An equation can be derived to calculate a correction to the pressure gradient needed in the two cross-stream momentum equations to give cross-stream velocity components that will satisfy continuity for each mesh region. The resulting equation resembles a finite-difference Poisson equation for pressure over the downstream cross section. This correction to the pressure gradient is needed to develop the correct cross flow within the boundary layer. Iteration is required at each station to satisfy both the continuity equation and the momentum equations.

If heat transfer is neglible, constant rothalpy may be assumed. The energy equation is used when heat transfer by convection and conduction is of interest. Then the rothalpy at the downstream station is calculated implicitly. Boundary conditions may specify adiabatic walls, specified wall temperature, or specified heat flux through the walls.

Cases of practical interest will have a turbulent layer, of course. For this purpose, the Baldwin-Lomax eddy-viscosity model is used (ref. 4). Provision is made for specifying a constant turbulent Prandtl number for the energy equation.

Numerical Examples

Several combinations of geometry, mesh, and flow conditions have been calculated for verifying the PARAMAR code. Most of this has been done for laminar flow to avoid the possibility of inaccuracy due to the turbulence model. Most of the geometry has been for straight ducts of various cross-sections, at varying angles, and for accelerating and decelerating flow. In addition some curved ducts and turbomachine blades have been run, which are given as examples below.

Laminar flow in a curved duct. - The duct is shown in figure 3. Laser velocimeter measurements have been made by Taylor, Whitelaw, and Yianeskis (ref. 12). The measurements and calculations were made at a Reynolds number of 790, based on the hydraulic diameter of the duct. The calculation was started at 0.1 m upstream of the start of the bend with uniform flow. The mesh used for the calculation by PARAMAR is shown in figure 4. The inviscid pressure field shown in figure 5 was obtained by using the Denton code (ref. 10). Some difficutly was had with negative velocities on the pressure surface near the start of the bend. There is a strong adverse pressure gradient in this region, as shown in figure 5, which resulted in negative streamwise velocities being calculated. These negative velocities are closer to the wall than the experimental measurements shown in Ref. 12. When the streamwise velocities become negative, the streamwise momentum is increased to a small value (2 percent of the freestream value for this case). Thus a small amount of momentum is being artificially added to the boundary layer. The added energy is negligible, but allows calculation through the small reverse flow region. This is a variation on the commonly used Reyhner and Flugge-Lotz approximation (ref. 13).

Carpet plots of streamwise velocities and cross-section vector plots are shown in figures 6 and 7. The results agree qualitatively with the experimental results. In order to make a detailed comparison with the experiment, it is necessary to impose the proper flow field at the start of the bend, which has not yet been done.

Flow through an axial stator. - The blade passage is shown in figure 8. A cusp has been added to the very blunt leading edge. Flow for this geometry has been calculated for laminar flow at a Reynolds number of 197, based on the upstream hydraulic diameter. An inviscid pressure field was obtained by the MERIDL and TSONIC codes (refs. 8 and 9). Calculated velocity magnitudes and cross-section vector plots are shown in figures 9 and 10. Although experimental comparisons have not yet been made, the results are qualitatively correct. An effort is being made to obtain a turbulent flow solution at a much higher Reynolds number.

REFERENCES

1. Patankar, S. V. and Spalding, D. B., "A Calculation Procedure for Heat, Mass and Momentum Transfer in Three-Dimensional Parabolic Flows," International Journal of Heat and Mass Transfer, Vol. 15, Oct. 1972, pp. 1787-1806.

2. Briley, W. R., and McDonald, H., "Three-Dimensional Viscous Flows with Large Secondary Velocity," Journal of Fluid Mechanics, Vol. 144, July 1984, pp. 47-77.

3. Davis, R. T., and Rubin, S. G., "Non-Navier Stokes Viscous Flow Computations," Computers and Fluids, Vol. 8, No. 1, Mar. 1980, pp. 101-131.

4. Baldwin, B. S. and Lomax, H., "Thin Layer Approximation and Algebraic Model for Separated Flows," AIAA Paper 78-257, Jan. 1978.

5. Steger, J. L., "Implicit Finite-Difference Simulation of Flow about Arbitrary Two-Dimensional Geometries," AIAA Journal, Vol. 16, No. 7, July 1978, pp. 679-686.

6. Pulliam, T. H. and Steger, J. L., "Implicit Finite-Difference Simulations of Three-Dimensional Compressible Flow," AIAA Journal, Vol. 18, No. 2, Feb. 1980, pp. 159-167.

7. Viviand, H., "Conservative Forms of Gas Dynamic Equations," La Recherche Aerospatiale, No. 158, Jan.-Feb. 1974, pp. 65-66.

8. Katsanis, T. and McNally, W. D., "Revised FORTRAN Program for Calculating Velocities and Streamlines on the Hub-Shroud Midchannel Stream Surface of an Axial-, Radial-, or Mixed-Flow Turbomachine or Annular Duct. I-Users Manual, " NASA TN-D-8430, 1977.

9. Katsanis, T., "FORTRAN Program for Calculating Transonic Velocities on a Blade-to-Blade Stream Surface of a Turbomachine," NASA TN-D-5427, 1969.

10. Denton, J. D., "An Improved Time Marching Method for Turbomachinery Flow Calculation," ASME Paper 82-GT-239, Apr. 1982.

11. Varga, R. S., Matrix Iterative Analysis, Prentice-Hall, New York, 1962.

12. Taylor, A. M. K. P., Whitelaw, J. H., and Yianneskis, M., "Curved Ducts with Strong Secondary Motion; Velocity Measurements of Developing Laminar and Turbulent Flows," Journal of Fluids Engineering, Vol. 104, No. 3, Sept. 1982, pp. 350-358.

13. Reyhner, T. A., and Flugge-Lotz, I., "The Interaction of a Shock Wave with a Laminar Boundary Layer," International Journal of Non-Linear Mechanics, Vol 3, 1968, pp. 173-199.

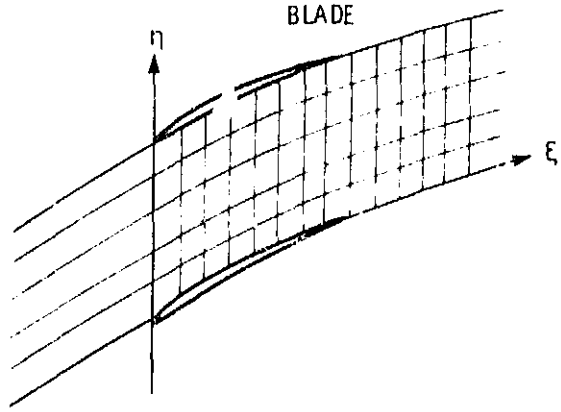

BLADE-TO-BLADE SURFACE

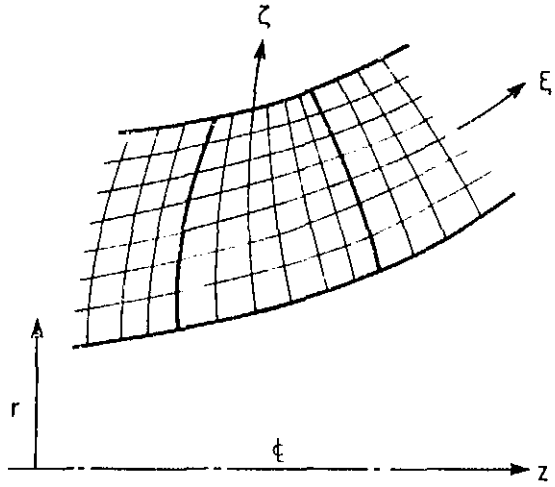

MERIDIONAL PLANE

Figure 1. - Mesh and coordinate system.

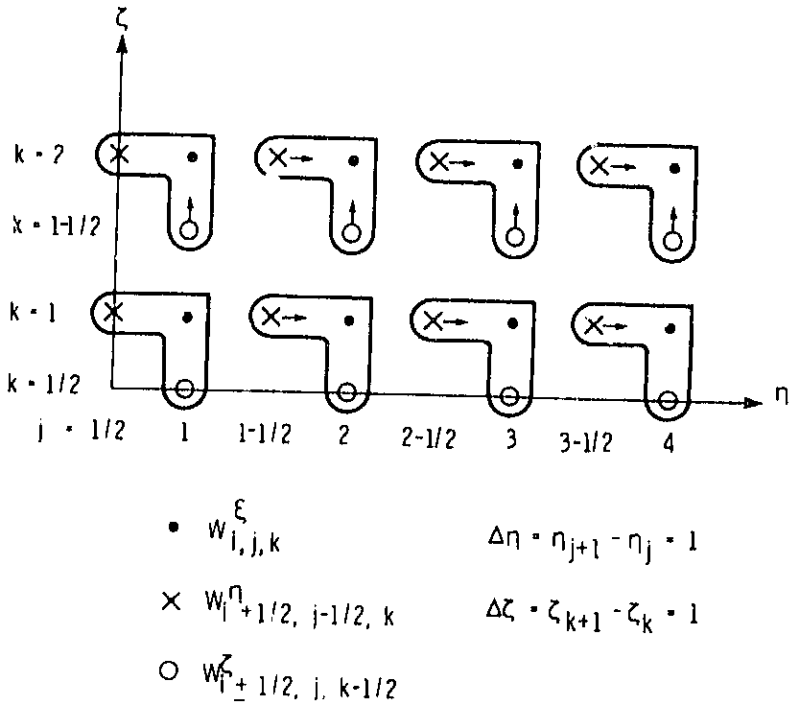

Figure 2. - Cross-section (η - ζ) surface. Mesh arrangement and numbering scheme for staggered grid.

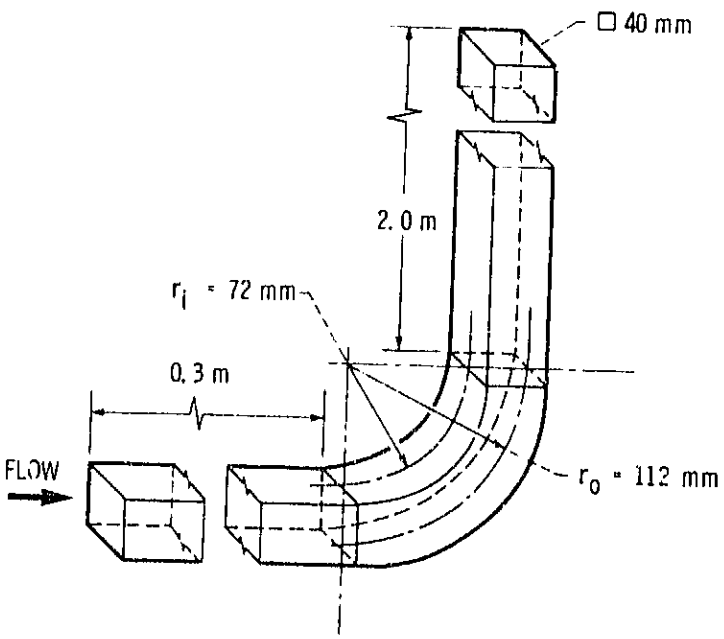

Figure 3. - Dimensions of curved duct.

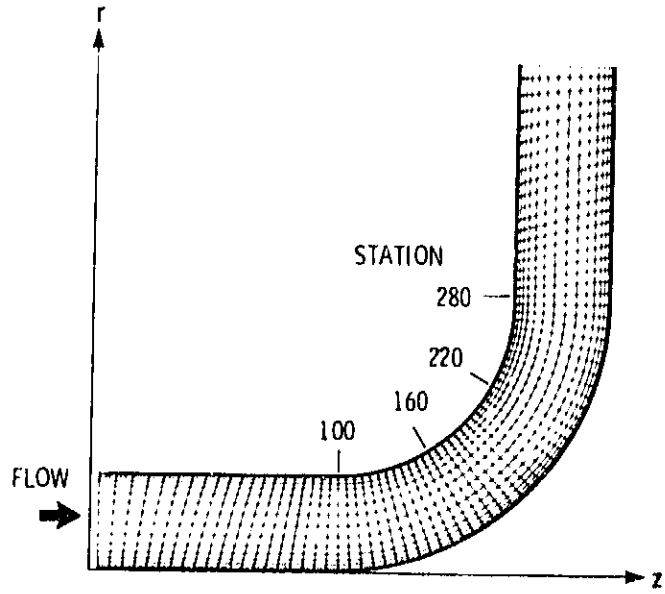

Figure 4. - Computational mesh for curved duct. Every fifth marching station shown. Every other streamwise mesh line shown.

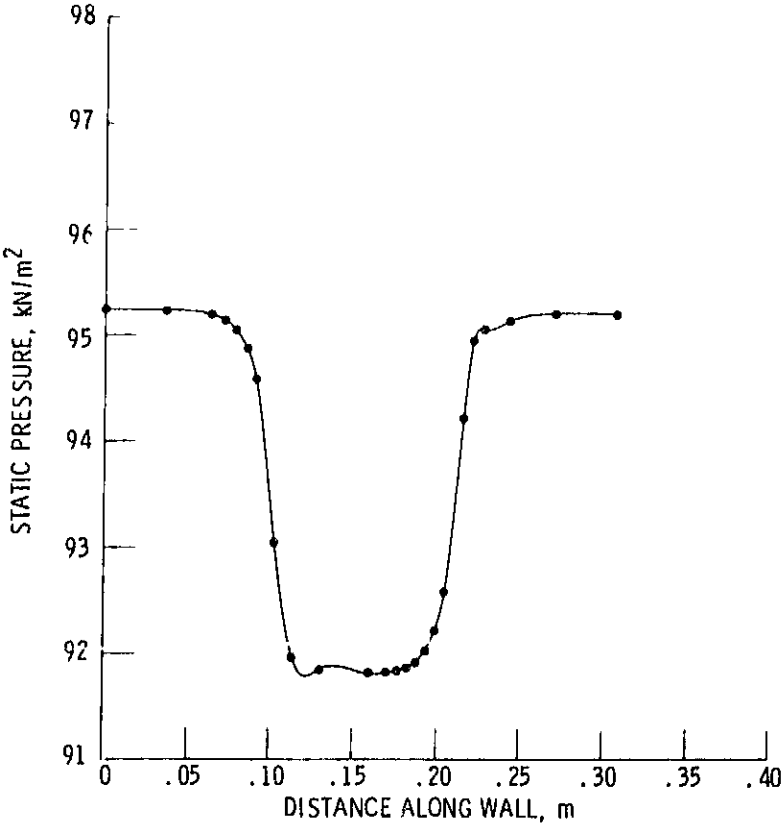

(a) Suction surface.

Figure 5. - Inviscid pressure for curved duct.

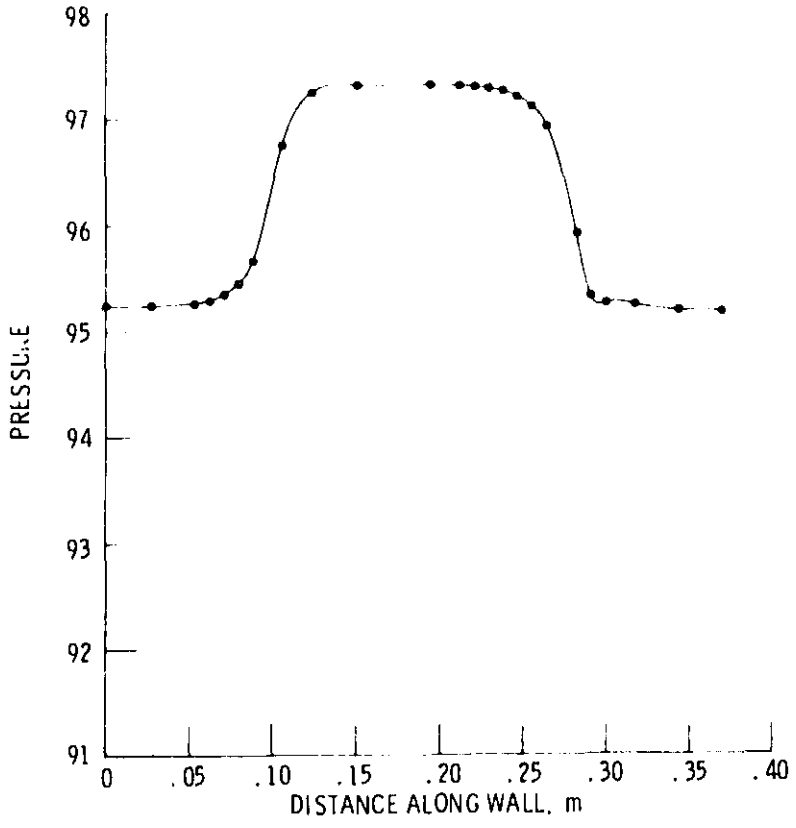

(b) Pressure surface.

Figure 5. - Concluded.

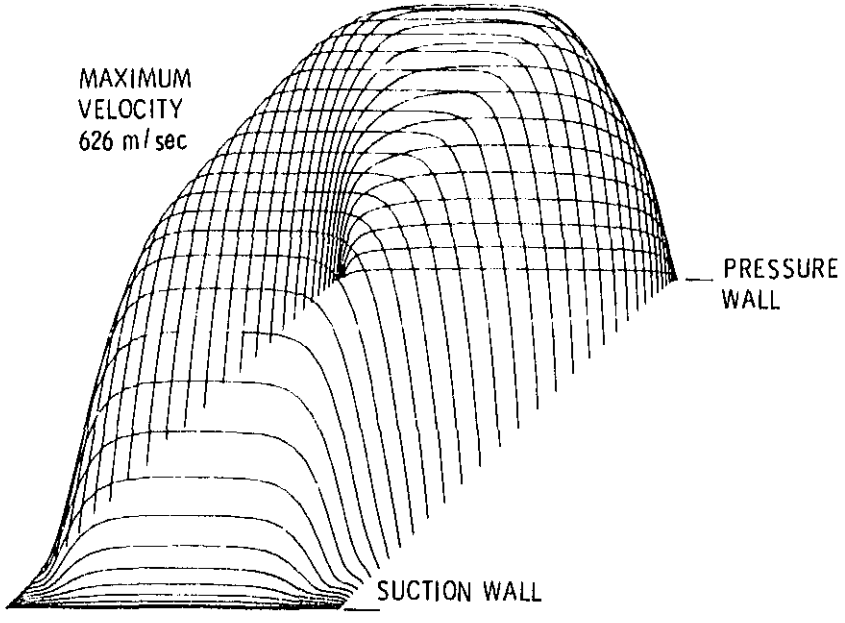

(a) Station 100. (See figure 4.)

Figure 6. - Streamwise velocities for curved duct.

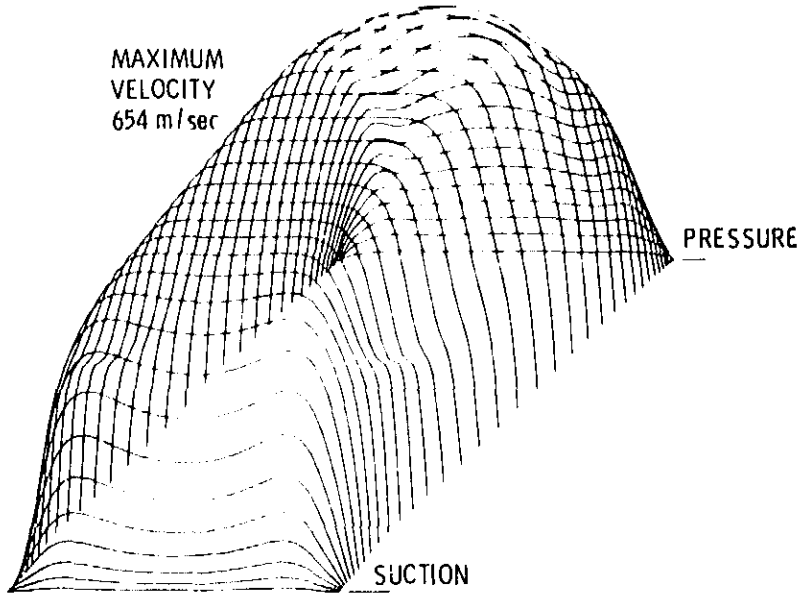

(b) Station 160.

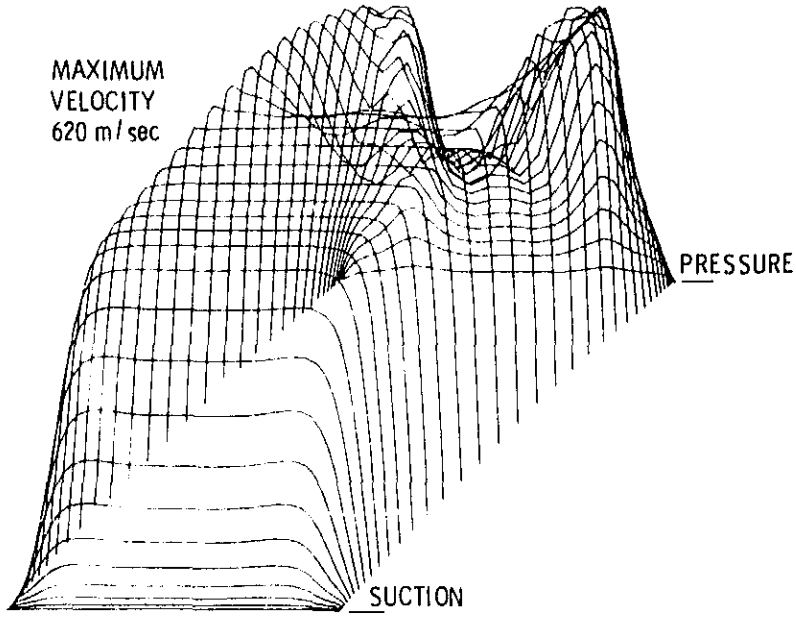

(c) Station 220.

Figure 6. - Continued.

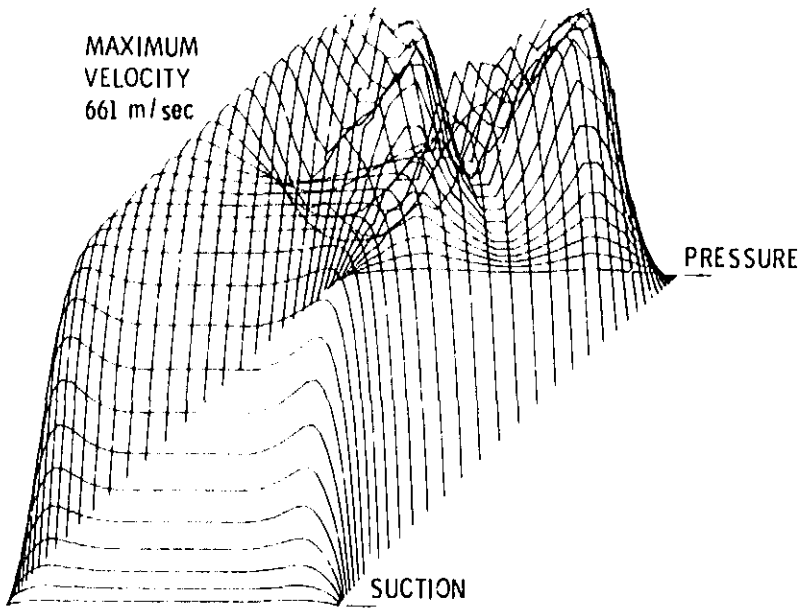

(d) Station 280.

Figure 6. - Concluded.

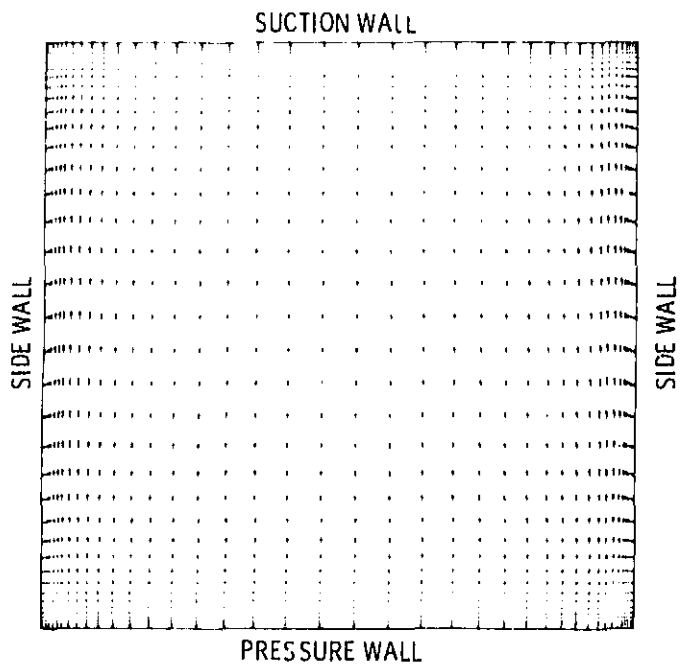

(a) Station 100. (See figure 4.)

Figure 7. - Secondary velocity vectors for cruved duct.

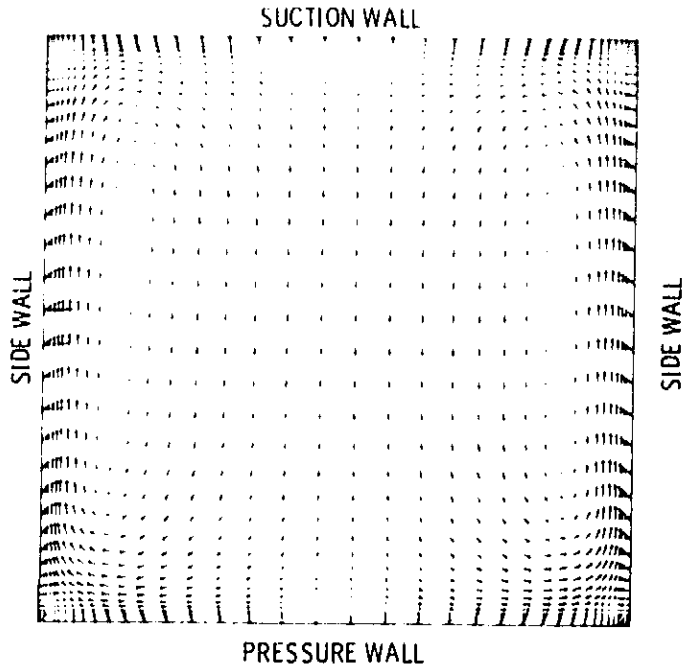

(b) Station 160.

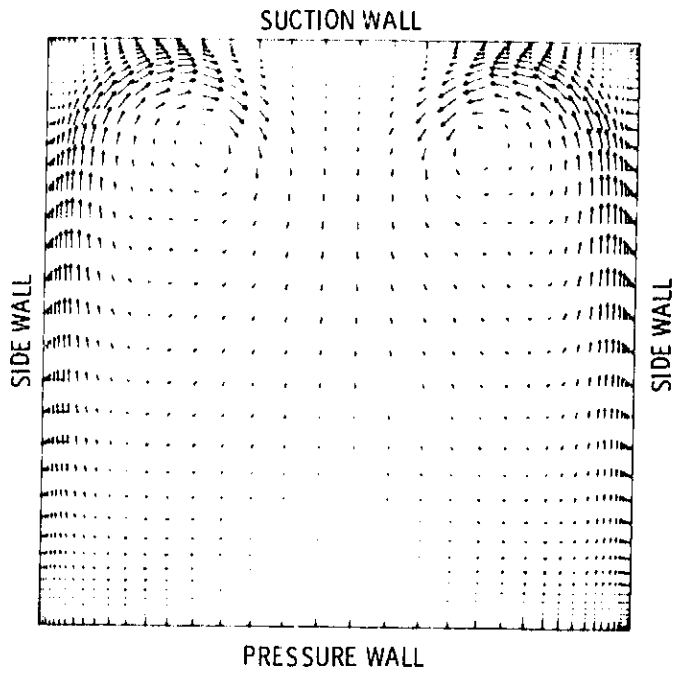

(c) Station 220.

Figure 7. - Continued.

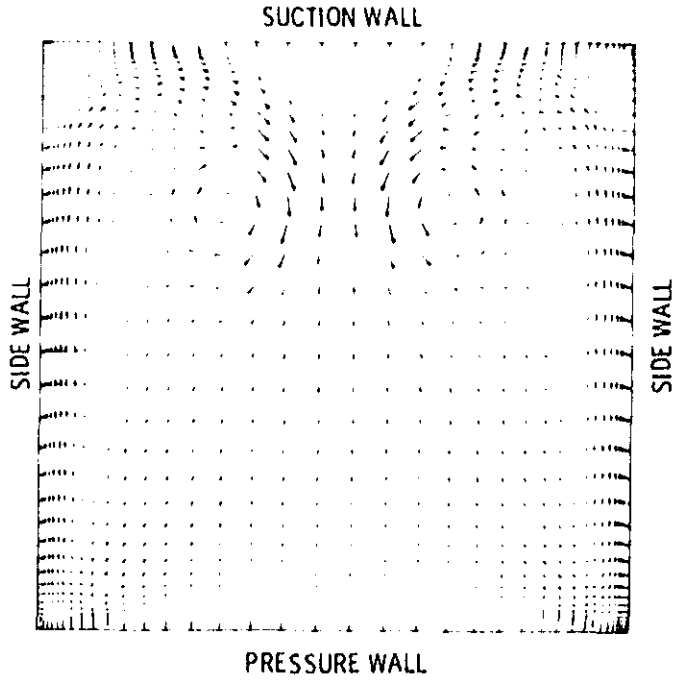

(d) Station 280.

Figure 7. - Concluded.

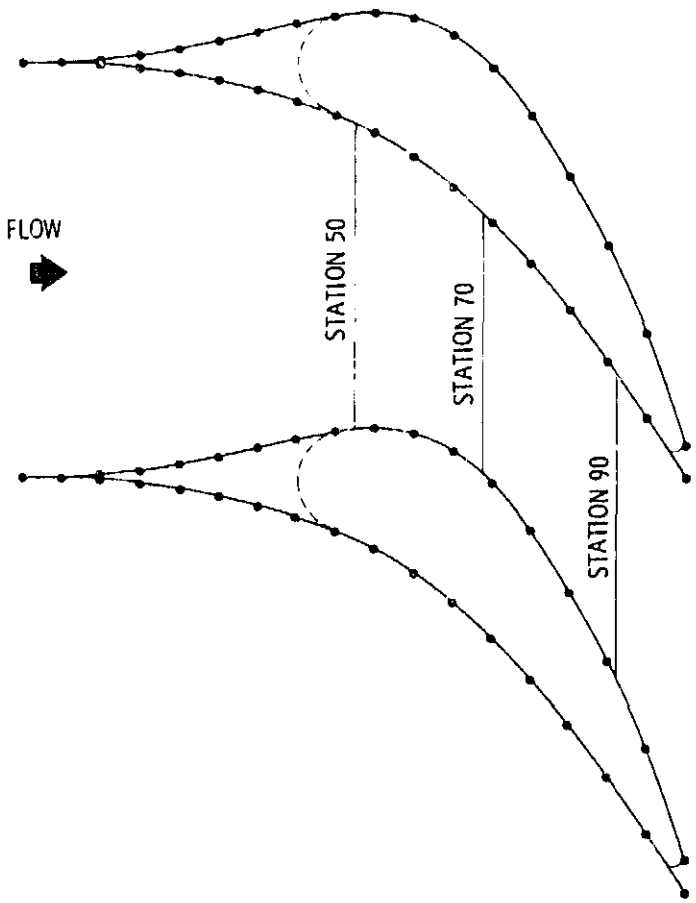

Figure 8. - Axial stator.

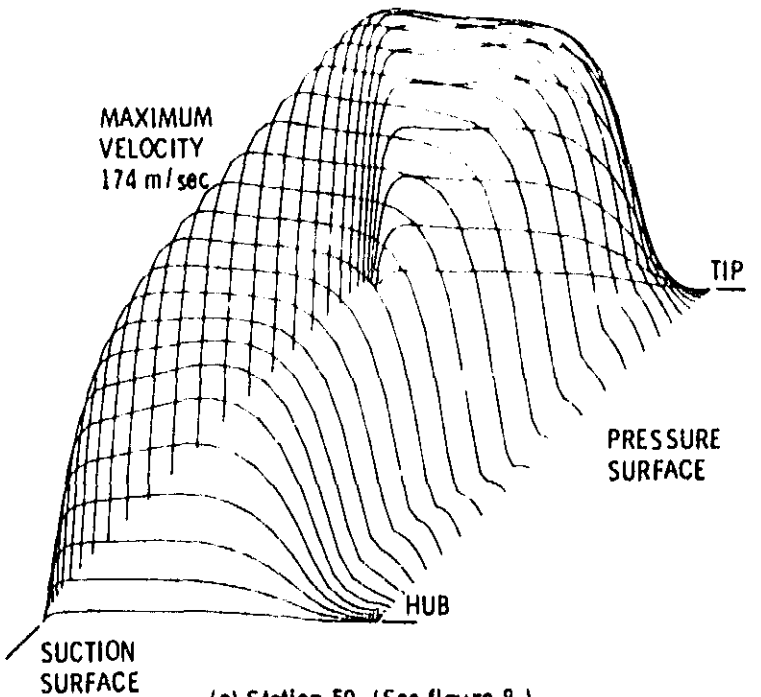

(a) Station 50. (See figure 8.)

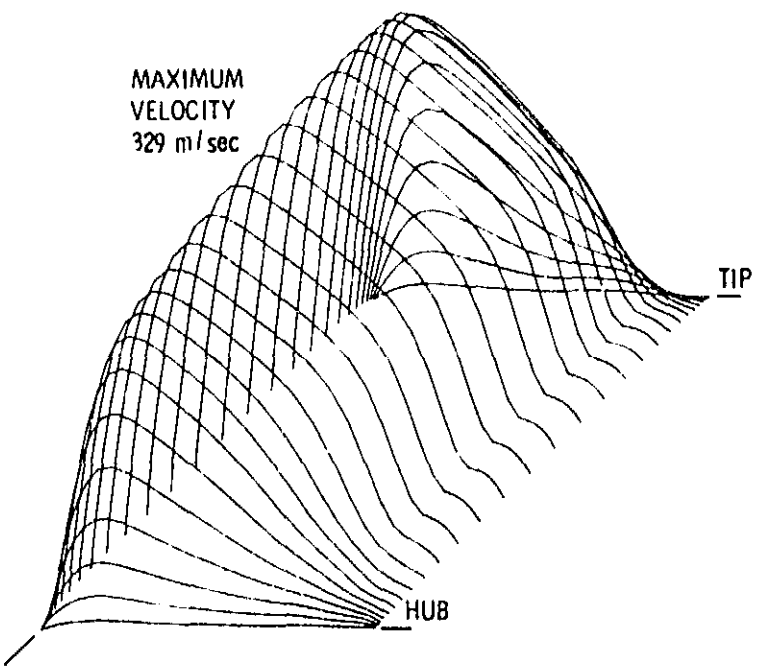

(b) Station 70.

Figure 9. - Velocity magnitudes for axial stator.

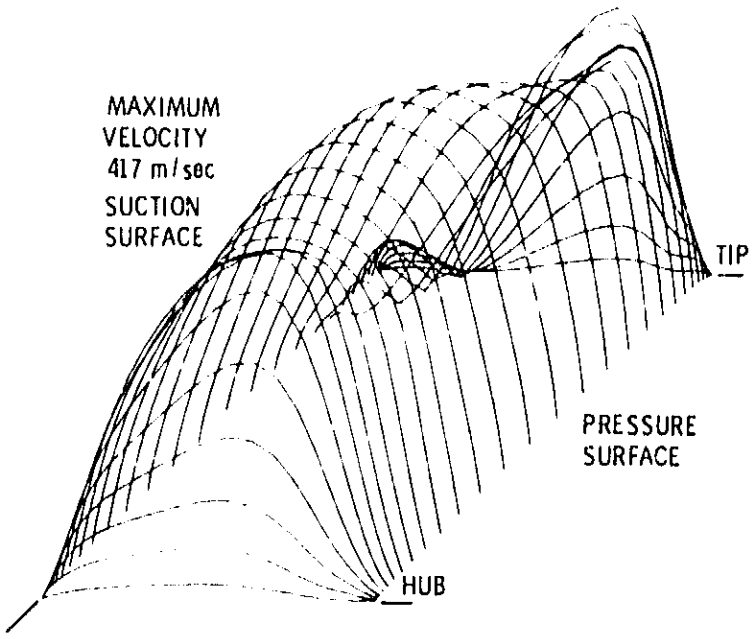

(c) Station 90.

Figure 9. - Concluded.

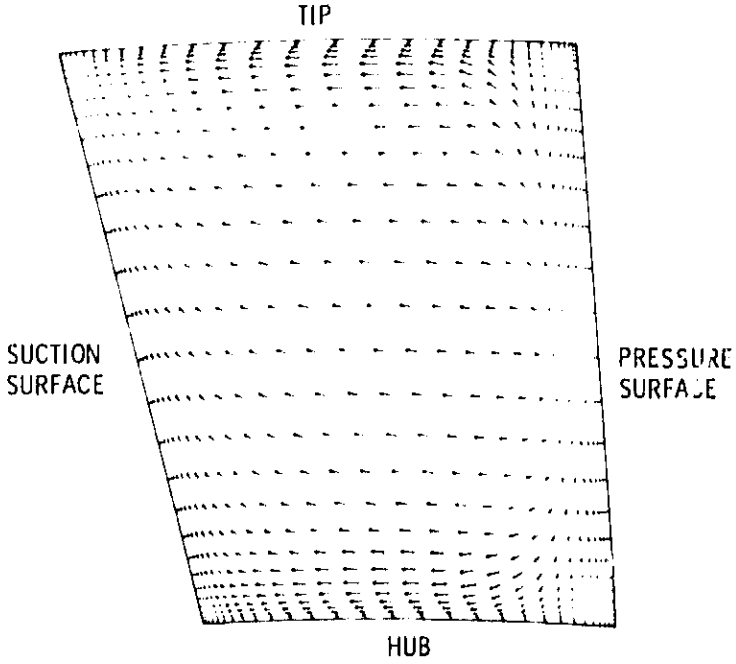

(a) Station 50. (See figure 8.)

Figure 10. - Secondary velocity vectors for axial stator.

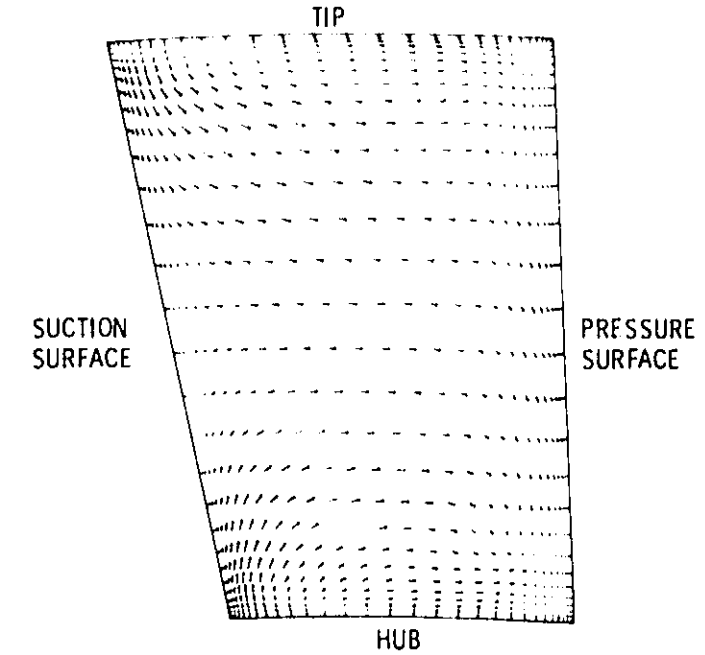

(b) Station 70.

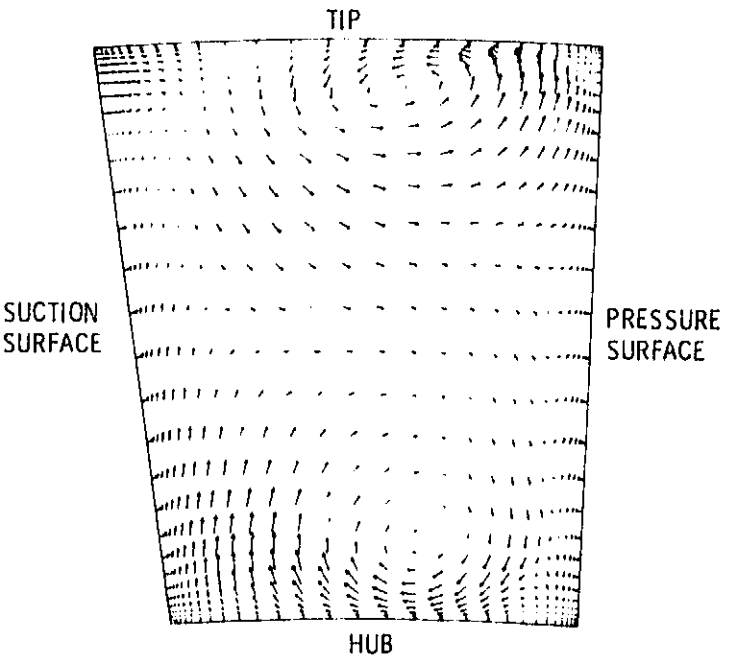

(c) Station 90.

Figure 10. - Concluded.